Title

Protein-induced membrane curvature alters local membrane tension.

Journal

Biophysical journal, 107(3)

ISSN

0006-3495

Authors

Rangamani, Padmini
Mandadap, Kranthi K
Oster, George

Publication Date

2014-08-01

DOI

10.1016/j.bpj.2014.06.010

Peer reviewed

Article

Protein-Induced Membrane Curvature Alters Local Membrane Tension

Padmini Rangamani,[1] Kranthi K. Mandadap,[1,2] and George Oster[1,*]
[1]Department of Molecular and Cell Biology and [2]Department of Chemistry, University of California at Berkeley, Berkeley, California

ABSTRACT Adsorption of proteins onto membranes can alter the local membrane curvature. This phenomenon has been observed in biological processes such as endocytosis, tubulation, and vesiculation. However, it is not clear how the local surface properties of the membrane, such as membrane tension, change in response to protein adsorption. In this article, we show that the partial differential equations arising from classical elastic model of lipid membranes, which account for simultaneous changes in shape and membrane tension due to protein adsorption in a local region, cannot be solved for nonaxisymmetric geometries using straightforward numerical techniques; instead, a viscous-elastic formulation is necessary to fully describe the system. Therefore, we develop a viscous-elastic model for inhomogeneous membranes of the Helfrich type. Using the newly available viscous-elastic model, we find that the lipids flow to accommodate changes in membrane curvature during protein adsorption. We show that, at the end of protein adsorption process, the system sustains a residual local tension to balance the difference between the actual mean curvature and the imposed spontaneous curvature. We also show that this change in membrane tension can have a functional impact such as altered response to pulling forces in the presence of proteins.

INTRODUCTION

Interaction of proteins with membranes is a fundamental biological process. Adsorption of proteins onto a membrane surface can induce curvature of the bilayer (1). There are many examples where this process is necessary for cellular functions: i.e., the binding of coat proteins that initiate endocytosis (2,3), scaffolding of the membrane by protein complexes such as eisosomes (4,5), and curvature sensing and modulation by the BAR domain family of proteins (1,2,6,7). In many of these instances, the proteins bind cooperatively to form complexes large enough that protein-complex diffusions are negligible, and so these complexes are essentially stationary (4,7,8). The intrinsic structure of these proteins induces the lipid bilayer to curve in such a way as to accommodate the shape of the protein (2,3,7,9). Changes in the membrane shape in response to protein binding have been documented in several ultrastructure studies (3,10). These experiments employ proteins to drive changes in the membrane curvature in order to mimic biological phenomena.

Global binding of proteins

Membrane surface properties change in response to protein binding. This has been studied using Langmuir troughs (11) and giant vesicles (12) where proteins covered the entire membrane. Binding of influenza virus fusion peptide with lipid monolayers produced a decrease in surface tension (11). Experiments using giant vesicles and video microscopy have shown that activity of bacteriorhodopsin pumps can reduce global membrane tension in the vesicles (12,13). In giant vesicles, this drop in tension was quantified using measurements of the fluctuation spectrum before and after the proteins were activated. This observation opens the question: what happens to the membrane tension when curvature-inducing proteins such as BAR domain proteins bind to the membrane?

The change in global membrane tension due to curvature-inducing proteins can be explained by a simple example. Consider a spherical vesicle of effective radius R, and membrane tension λ, as shown in Fig. 1 *A*. The relationship between R and λ is given by the capillarity equation $\Delta p - 2\lambda/R = 0$, where Δp is the osmotic pressure difference between the inside and outside of the vesicle. Note that these vesicles are not taut and have an area fraction that is microscopically unresolvable, but serves as a lipid reservoir. The value of the unresolvable area fraction depends on the bending modulus of the membrane and has been estimated to be 1.5% (14). This area fraction is sufficient to allow the change in the effective vesicle radius when proteins bind to it. If this vesicle is now coated everywhere with proteins with spontaneous curvature C, then the new vesicle radius changes to R_{new}. If the osmotic pressure difference remains unchanged, we can write $\Delta p - 2\lambda_{\text{new}}/R_{\text{new}} = 0$. Therefore, the membrane tension of the vesicle changes due to the spontaneous curvature of the proteins binding everywhere to the vesicular membrane.

Local binding of proteins

In cells, proteins are known to bind to membranes locally, usually to initiate or regulate a biological function (2–5).

Submitted February 26, 2014, and accepted for publication June 9, 2014.

*Correspondence: goster@berkeley.edu

Editor: Sean Sun.

0006-3495/14/08/0751/12 $2.00

http://dx.doi.org/10.1016/j.bpj.2014.06.010

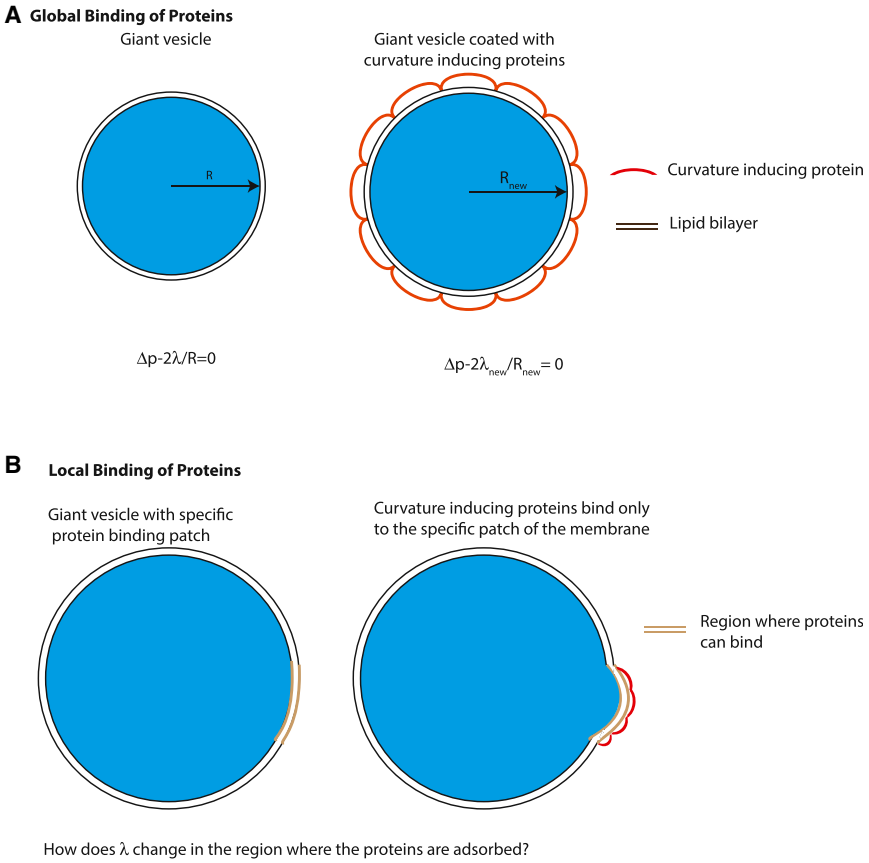

FIGURE 1 Proteins can bind to membranes globally or locally. (*A*) When proteins bind to the membrane globally, the capillarity equation can be used to explain the change in membrane tension. In this simplified schematic, we are not showing the microscopically unresolvable area fraction of the lipids that is absorbed by undulations. However, we assume that this area fraction serves as a lipid reservoir. (*B*) When proteins bind only to a specific region in the vesicle, how can we explain the changes in λ? To see this figure in color, go online.

These processes can be understood using lipid vesicles with lipid domains that can bind specific proteins (Fig. 1 *B*). Using these systems, several groups have shown that protein adsorption on lipid domains can alter the lateral pressure profile on the bilayer and induce tubulation (6,15). In Stachowiak et al. (6) and Zhao et al. (16), the authors use GFP-tagged proteins that adsorbed onto the bilayer. These proteins raised the lateral surface pressure and induced tubules to sprout from lipid vesicles. The formation of buds can also be studied using this experimental setup (17). This raises the question of how the membrane properties are altered when proteins bind to specific local domains rather than globally. Recently, the Helfrich potential energy was used to show that adsorbed proteins give rise to spontaneous surface tension (15). It is not clear, however, how adsorption of proteins to small regions on the membrane surface alters the properties of the lipid bilayer, nor how the lipids flow to accommodate the shape change of the membrane. In this study, we present a continuum mathematical model, along with numerical simulations, of a lipid bilayer under the influence of a patch of curvature-inducing proteins.

Continuum modeling of biological membranes

Biological membranes have unique mechanical properties. In an aqueous medium, lipids aggregate into quasi-two-dimensional bilayer sheets and adopt a configuration that minimizes the exposure of their hydrophobic parts. Even a plain lipid bilayer displays strange mechanical behaviors. In the plane of the membrane, it resembles a nearly incompressible viscous fluid, although in bending it behaves somewhat like an elastic solid. In-plane lipid flow has been observed in experimental systems such as tether formation and micropipette aspiration of membranes (18). In cellular processes, the plasma membrane is thought to have a membrane reservoir that can act as a source of lipids (19). This reservoir allows for lipid flow during dynamic events such as spreading, motility, and endocytosis (19). Although the idea of lipid flow on the surface of membranes has been explored previously (20,21), most of these models focused only on lipid flow in a cell or a vesicle of fixed shape.

Hydrodynamics in membrane systems, in general, must include the viscosity of the surrounding bulk fluid (22,23), the in-plane flow of lipids (22,24–26), and intermonolayer friction (22–24,26). As shown in Seifert and Langer (22), Rahimi and Arroyo (26), and Sens (27), each of these viscosities sets a different timescale for the membrane dynamics. In particular, for relaxation from fluctuations, the timescale set by bulk viscosity and intermonolayer friction is important (22). Here, we study the lipid flow on the membrane surface required to accommodate shape changes and

surface area due to curvature induced by protein adsorption. For this, the relevant timescale for shape change and curvature is set by the surface viscosity of the membrane (26).

Motivation

Simultaneous lipid flow and membrane shape change is a complex phenomenon. The coupling between the change in membrane shape induced by protein adsorption and the corresponding change in membrane surface properties is not yet fully understood. This calls for a model that can describe such coupling. Furthermore, because asymmetry is one of the hallmarks of biological structures, it is important that such a model not be restricted to axisymmetric geometries. Here, we develop a two-dimensional model that can capture local inhomogeneities in the membrane properties in response to protein-adsorption. Using this two-dimensional model, we show how the local tension of the membrane changes in response to protein adsorption and how this drives surface flow of the membrane's constituent lipids. We also show that the Helfrich elastic model results in a complicated integro-differential equation that captures the change in local membrane tension in two-dimensional geometries (see Section S2 in the Supporting Material). This equation is difficult to solve both analytically and numerically; it can be solved easily for axisymmetric calculations, as shown in Lipowsky (15).

The article is organized as follows: In Viscous Elastic Model, we propose a two-dimensional viscous-elastic formulation of lipid membrane dynamics that accounts for local spontaneous curvature due to protein adsorption. In Results, using numerical simulations, we show that changes in the local spontaneous curvature due to protein adsorption alters the local tension. Moreover, lipids flow from the boundaries to accommodate the changes in membrane curvature. We also study the effects of protein adsorption on the response of the membrane to a pulling force. In Discussion and Conclusions, we elaborate on the results from the simulations and their relevance to protein-adsorption phenomena and biological function.

Viscous Elastic Model

Assumptions

1. The lipid bilayer is modeled as a two-dimensional differentiable manifold endowed with the appropriate mechanical and material properties. Helfrich proposed a model that treats the manifold as an elastic shell whose bending behavior is captured by an energy density functional that depends only on the manifold's local curvatures (28). Models of this sort proved sufficient for radii of curvatures much larger than the membrane thickness, and rich geometric behavior could be obtained by minimizing the elastic bending energy.
2. The lipid bilayer is assumed to be incompressible, based on the large stretch modulus (29). This constraint is introduced using a Lagrange multiplier γ (see Table 1 for notation).
3. Lipid flow is modeled using an intrasurface viscosity (25). (Note that although interleaflet friction and external fluid viscosity are both important for modeling the hydrodynamics, we do not include them in this model.)
4. Protein adsorption on the membrane is captured using a spontaneous curvature (C). A lipid bilayer has two separate interfaces, whereas the simple manifold model has but one. Still, one can introduce the notion of an intrinsic curvature due to, say, different lipids or proteins on each leaflet, and thus rescue the Helfrich model by including this built-in curvature (15,28).

We revisit these assumptions in Discussion and Conclusions, and relate the strengths and shortcomings of our model.

Kinematics

We use a Monge parameterization to describe the manifold representing the membrane (also see Table 1). The position of a point on the membrane is given by

$$\begin{aligned}\mathbf{r} &= x_\alpha \mathbf{e}_\alpha + z(x_1, x_2, t)\mathbf{e}_3,\\ \alpha &\in \{1,2\},\end{aligned} \tag{1}$$

where $\mathbf{e}_1$, $\mathbf{e}_2$, and $\mathbf{e}_3$ are the orthonormal coordinate axes (see Fig. 2). The natural tangent bases on the membrane are $\mathbf{a}_\alpha = \mathbf{r}_{,\alpha} = \mathbf{e}_\alpha + z_{,\alpha}\mathbf{e}_3$, where $(\,)_{,\alpha}$ represents the partial derivative with respect to x^α. The components of the induced metric and curvature tensors in this parameterization are given by

$$a_{\alpha\beta} = \mathbf{a}_\alpha \cdot \mathbf{a}_\beta = \delta_{\alpha\beta} + z_{,\alpha} z_{,\beta}, \tag{2}$$

$$b_{\alpha\beta} = \mathbf{n} \cdot \mathbf{r}_{,\alpha\beta} = z_{,\alpha\beta} \big/ \sqrt{a}, \tag{3}$$

TABLE 1 Notation used in developing the viscous elastic model

Notation	Description	Units
W	Local energy per unit area	pN/nm
$\mathbf{r}$	Position vector	—
$\mathbf{n}$	Normal to the membrane surface	unit vector
$\mathbf{a}_\alpha$	Basis vectors describing the tangent plane, $\alpha \in \{1,2\}$	—
γ	Lagrange multiplier for the incompressibility constraint	pN/nm
λ	$-(W+\gamma)$	pN/nm
w	Normal component of the velocity vector	—
$\mathbf{V}$	Tangential velocity vector	—
p	Pressure difference across the membrane	pN/nm^2
H	Mean curvature of the membrane	nm^{-1}
K	Gaussian curvature of the membrane	nm^{-2}
k	Bending modulus	pN·nm
$\bar{k}$	Gaussian modulus	pN·nm
ν	Intrasurface viscosity	pN·s/nm

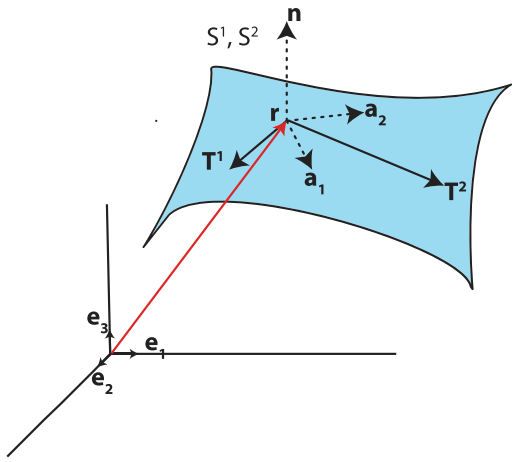

FIGURE 2 The tangent basis $\mathbf{a}_1$ and $\mathbf{a}_2$ can be constructed at any point on the membrane as $\mathbf{a}_\alpha = \mathbf{r}_{,\alpha}$, where $\mathbf{r}$ is the position given by Eq. 1 and $\alpha \in \{1,2\}$. The surface normal $\mathbf{n}$ is then $\mathbf{a}_1 \times \mathbf{a}_2/|\mathbf{a}_1 \times \mathbf{a}_2|$. The tangential components of the stress vectors $\mathbf{T}^1$ and $\mathbf{T}^2$ lie on the surface whereas the normal components S^1 and S^2 are along the surface normal. The total stress vectors are given by $\boldsymbol{\sigma}^1 = \mathbf{T}^1 + S^1\mathbf{n}$ and $\boldsymbol{\sigma}^2 = \mathbf{T}^1 + S^2\mathbf{n}$. The definitions of $\mathbf{T}^\alpha$ and S^α are given in the Supporting Material and by Rangamani et al. (25). To see this figure in color, go online.

respectively (30). Here, $a = \det(a_{\alpha\beta})$, and

$$\mathbf{n} = \frac{\mathbf{e}_3 - z_{,\alpha}\mathbf{e}_\alpha}{\sqrt{a}}$$

is the membrane normal. The dual metric and dual curvature components are given by

$$a^{\alpha\beta} = (a_{\alpha\beta})^{-1} \text{ and}$$

$$b^{\alpha\beta} = a^{\alpha\lambda}a^{\beta\mu}b_{\lambda\mu},$$

respectively.

The velocity of any point $\mathbf{r}$ on the membrane may be decomposed into tangent and normal components as

$$\mathbf{v} = \dot{\mathbf{r}} = v^\alpha\mathbf{a}_\alpha + w\mathbf{n}, \tag{4}$$

where v^α are the intramembrane flow velocities and $w = z_{,t}/\sqrt{a}$ is the normal velocity of the membrane.

Free energy of membranes with protein adsorption

Protein adsorption onto the membrane induces a change in the local curvature of the membrane. This can be modeled by using a modified local form of the Helfrich energy density per unit area given by (28)

$$W = k(H - C)^2 + \overline{k}K, \tag{5}$$

where

$$H = 1/2a^{\alpha\beta}b_{\alpha\beta} \text{ and}$$

$$K = 1/2\varepsilon^{\alpha\beta}\varepsilon^{\lambda\mu}b_{\alpha\lambda}b_{\beta\mu}$$

are the mean and Gaussian curvatures, respectively; $\varepsilon_{\alpha\beta}$ is the permutation tensor; and k and $\overline{k}$ are the corresponding bending moduli. $C(x^1,x^2)$ is the spontaneous curvature induced by the proteins. The difference between our form of the energy and the Helfrich energy is a factor of one-half, which is just a constant carried through all the calculations.

Equations of motion

With this machinery, we now develop a model for lipid bilayers with surface flow in the presence of protein-induced spontaneous curvature. The equations of motion in the absence of inertia are simply the equations of mechanical equilibrium. The force balance on the membrane, subjected to a net lateral pressure p in the direction of the local surface unit normal $\mathbf{n}$, can be summarized in the compact form (31) (see also Section S1 in the Supporting Material)

$$\boldsymbol{\sigma}^\alpha_{;\alpha} + p\mathbf{n} = 0, \tag{6}$$

$$\begin{aligned}\boldsymbol{\sigma}^\alpha &= \mathbf{T}^\alpha + S^\alpha\mathbf{n},\\ \alpha &\in \{1,2\},\end{aligned} \tag{7}$$

where $(\,)^\alpha_{;\alpha}$ is the covariant divergence; $\boldsymbol{\sigma}^\alpha$ values are the stress vectors; and $\mathbf{T}^\alpha$ values are tangential stress vector fields that are constitutively determined, and depend on the energy per unit mass of the membrane. S^α is a contravariant vector field that contains the normal component of the stress vector (25,31). We use a balance law formulation (see Rangamani et al. (25)) to derive the equations of motion for a membrane with intrasurface flow in the presence of curvature inducing proteins. This approach has two distinct advantages over the commonly used global energy minimization approach:

1. The local stress balance approach allows us to account for local inhomogeneities in the membrane (see Steigmann (31) for a detailed explanation).
2. The local force balance allows us to include dissipation arising from intramembrane viscosity; the viscous stress contributes to $\mathbf{T}^\alpha$ only, i.e., including in-plane flow of lipids affects only the tangential stress terms (25,26).

The membrane is assumed to be incompressible, which results in the following constraint (25):

$$\mathbf{div}\,\mathbf{v} - 2wH = 0. \tag{8}$$

The incompressibility constraint is implemented using a Lagrange multiplier γ (25,32).

Following the procedure in Rangamani et al. (25) and as shown in the Supporting Material, the equation of motion in the normal direction is

$$\underbrace{k\left[\Delta(H-C)+2(H-C)\left(H^2+HC-K\right)\right]-2\lambda H}_{\text{Elastic contribution}} + \underbrace{2\nu\left[b^{\alpha\beta}d_{\alpha\beta}-w\left(4H^2-2K\right)\right]}_{\text{Viscous contribution}} = p. \tag{9}$$

The equations of motion in the tangent plane are

$$\lambda_{,\gamma}-4\nu w H_{,\gamma}+2\nu\left(a^{\alpha\mu}d_{\gamma\mu;\alpha}-w_{,\alpha}b^{\alpha}_{\gamma}\right) = 2k(H-C)\frac{\partial C}{\partial x^{\gamma}}. \tag{10}$$

Here, $\Delta(\bullet)=(\bullet)_{,\alpha\beta}a^{\alpha\beta}$ is the surface Laplacian, ν is the membrane viscosity, $\lambda=-(W+\gamma)$, and

$$d_{\alpha\beta} = 1/2(v_{\alpha;\beta}+v_{\beta;\mu}), \tag{11}$$

$$v_{\alpha;\beta} = v_{\alpha,\beta}-v_{\phi}\Gamma^{\phi}_{\alpha\beta}. \tag{12}$$

Here, v_{α} are the covariant components of the velocity vector, $(\ )^{\alpha}$; is the covariant derivative, and $\Gamma^{\phi}{}_{\alpha\beta}=z_{\phi}z_{,\alpha\beta}/a$ indicates the Christoffel symbols (30) (see Section S1 in the Supporting Material for a complete derivation of the above equations). Moreover, γ is a Lagrange multiplier required to implement the area incompressibility constraint (Eq. 8, and see Eq. S15 in the Supporting Material), and is defined as the surface pressure of the membrane (25). This interpretation is consistent with the notation used in Jenkins (32).

Changes in the membrane shape in response to protein adsorption are obtained by solving Eqs. 8–10 along with appropriate boundary conditions (25).

Reduction to an elastic model

When the membrane viscosity, ν, is zero, the above model reduces to the elastic model of bilayer membranes. Therefore, Eq. 9 reduces to the well-known shape equation for the Helfrich energy (31)

$$k\left[\Delta(H-C)+2(H-C)\left(H^2+HC-K\right)\right]-2\lambda H = p. \tag{13}$$

The spatial variation of λ (10) in the elastic model is given by

$$\lambda_{,\gamma} = -\frac{\partial W}{\partial x^{\gamma}}\bigg|_{\text{exp}} = 2k(H-C)\frac{\partial C}{\partial x^{\gamma}}, \tag{14}$$

where *exp* denotes the explicit derivative of W with respect to the coordinates. In the absence of bending and spontaneous curvature, the force normal to any curve is given by $f_v=\lambda=-\gamma$ (see Rangamani et al. (25)), and therefore λ can be understood as the tension in a flat membrane. Furthermore, in the special case of zero spontaneous curvature and nonzero mean curvature, $\lambda=$ constant, everywhere (see Eq. 14). This constant value of λ must be provided as an input parameter to solve the system of equations (31), and is widely interpreted to be surface tension in Derényi et al. (33).

An intuitive explanation

The main outcome of the model is summarized in Eq. 14. Underneath the mathematical structure of the model is a simple, intuitive explanation for why membranes are able to sustain a surface tension gradient. Compare a lipid vesicle to a soap film: the main difference between the soap bubble and the membrane vesicle, at the continuum level, is the ability of lipid membranes to resist bending. That is, lipid bilayers have a finite bending modulus, whereas soap bubbles have zero bending modulus. If there was a gradient in tension between two different regions in a soap bubble, it would dissipate by virtue of Marangoni flow. However, in the case of bilayers, their ability to bend sustains the surface tension gradient, even after flow is dissipated (see Eq. 14). Therefore, lipid membranes are able to sustain the change in tension in the protein patch simply due to their ability to resist bending.

Interpretation of membrane tension

Membrane tension can be estimated from studying vesicles in vitro using several different approaches, as follows:

1. Capillary methods,
2. Fluctuation spectra of vesicles, and
3. Membrane tethering experiments.

In capillary methods, the vesicle diameter and the osmotic pressure difference between the exterior and the interior of the vesicle can be controlled. Because the vesicle is a sphere with constant mean and Gaussian curvatures, we can use the Young-Laplace equation resulting from the simplifications of Eq. 13 to obtain λ (see Phillips et al. (34) for a detailed explanation). Estimates of membrane tension can also be obtained from analysis of the fluctuation spectra of giant unilamellar vesicles using high-resolution contour detection techniques (35). Alternatively, in membrane tethering experiments, one can pull out tubes and measure the force versus length curves to obtain surface tension as parameter fits to the theory in Derényi et al. (33). Instead of using λ, one can use the surface pressure, γ, as a dependent variable. This introduces the Gaussian modulus into Eqs. 9 and 10. However, Gaussian moduli measurements vary widely in experiments (36,37), and can only be calculated accurately from simulations (38). Using λ is useful because it can be inferred from experiments on large spherical vesicles where the force normal to a boundary is

$$f_v = \lambda = \frac{p}{2H},$$

and where p is the pressure difference and H is the mean curvature. Hence, this value of λ can be used as a boundary condition to solve Eq. 10. In general, however, λ is not a uniform field and must be solved for simultaneously with the

shape of the membrane using the above model. Because λ is nonhomogeneous and depends on the local inhomogeneities, herein we refer to it as the local tension in the membrane.

Spontaneous tension as a special case

Here, we compare our work to the notion of spontaneous tension introduced in Eq. 15 to model proteins or solute particles that adsorb onto the lipid membrane and show that it is a special case of the elastic model presented in Reduction to an Elastic Model. In Eq. 15, the effect of adsorbed proteins is modeled by means of a spontaneous curvature, as in this work, where the total energy is given by (28)

$$\mathcal{W} = \int W \, dA = \int \left(k(H-C)^2 + \bar{k}K\right) dA. \tag{15}$$

In Eq. 15, the author considers a case when the resultant mean and Gaussian curvatures are significantly smaller than the applied spontaneous curvature in a certain area A_c:

$$\begin{aligned} H &\ll C, \\ K &\ll C^2. \end{aligned} \tag{16}$$

Therefore, the total energy in the area A_c is given by

$$\mathcal{W} \approx \int_{A_c} kC^2 \, dA = kC^2 A_c. \tag{17}$$

Thus, the effect of spontaneous curvature can be understood as an apparent constant tension λ_{sp} over the area A_c given by

$$\lambda_{sp} = \frac{\delta \mathcal{W}}{\delta A_c} = kC^2. \tag{18}$$

Equation 18 is the central result in Eq. 15. In the elastic model limit presented in our work, specializing to the case where Eq. 16 is true, we have from Eq. 14 that

$$\lambda_{,\gamma} \approx 2k(-C)\frac{\partial C}{\partial x^\gamma} = -\left(kC^2\right)_{,\gamma}. \tag{19}$$

Integrating Eq. 19 gives

$$\lambda\left(x^1, x^2\right) - \lambda\left(x_0^1, x_0^2\right) = -kC^2, \tag{20}$$

where $(x_0{}^1, x_0{}^2)$ is any point outside the protein patch. This tells us that the local tension differs between the protein patch and the rest of the membrane. This value is the spontaneous tension kC^2 as in Eq. 18. Hence, the result in Eq. 15 is a special case of the theory under the assumptions of Eq. 16. Finally, from the general viscous-elastic model, we find that the conditions imposed in Eq. 16 do not hold in general. For example, in the case where $C = 0.008$ nm^{-1}, the spatial values of the spontaneous and mean curvature are shown in Fig. S1, *A* and *B*, in the Supporting Material.

RESULTS

Effects of protein-induced spontaneous curvature

There are many protein complexes that bind to the membrane at specific sites and do not disperse (2,4–6). Therefore, we shall assume that proteins adsorb onto a small patch on the membrane and do not diffuse (39). The total system we study is 1000-nm square, with a preferred protein-binding patch of 50 nm in the center. The spontaneous curvature $C(x^1, x^2, t)$ generated by the proteins is assumed to be approximately uniform in the square patch and modeled as

$$\begin{aligned} C\left(x^1, x^2, t\right) = {} & 1/4 C_0(t)\left[\tanh\left(x^1 - 25\right) - \tanh\left(x^1 + 25\right)\right] \\ & \times \left[\tanh\left(x^2 - 25\right) - \tanh\left(x^2 + 25\right)\right], \end{aligned} \tag{21}$$

where $C_0(t)$ is the magnitude of the spontaneous curvature, which depends on the protein density (6) (see Fig. S1 *A*). The kinematic boundary conditions for the membrane position along the edges of the square patch are

$$\begin{aligned} z &= 0, \\ \mathbf{n} &= \mathbf{e}_3. \end{aligned} \tag{22}$$

We model the square patch as two closed boundaries (top and bottom) with no-slip boundary conditions on the tangential velocity field. The left and right boundaries are open to allow for lipid flow based on the following traction boundary conditions, which are themselves based on the general expressions for the edge forces (25):

$$\begin{aligned} 1/4 k z_{,11}^2 &= \nu v_{1;1}, \\ v_{2;1} + v_{1;2} &= 0. \end{aligned} \tag{23}$$

Additionally, the value of λ is specified on the open boundaries as $\lambda_0 = 5 \times 10^{-4}$ pN/nm (12,15,35). The other parameters used in the model are given in Table 2.

Proteins adsorb in the center of the patch. Therefore, we model $C_0(t)$ as a linear function of time as shown in Fig. 3 *A*. This function captures the increasing density of proteins that are absorbed onto the membrane over time. In this work, we only consider the dilute limit of proteins where the spontaneous curvature generated by the protein may be linearly proportional to the density of proteins. The nonlinear effects can be modeled by using the procedure shown in Zhu et al. (40). The partial differential equations are solved using finite-element methods (41–44) in the software

TABLE 2 Parameters used in the model

Parameter	Value	Reference
λ_0	5×10^{-4} pN/nm	(12,15,35)
k	82 pN•nm	(49)
ν	1×10^{-4} pN•s/nm	(50,51)

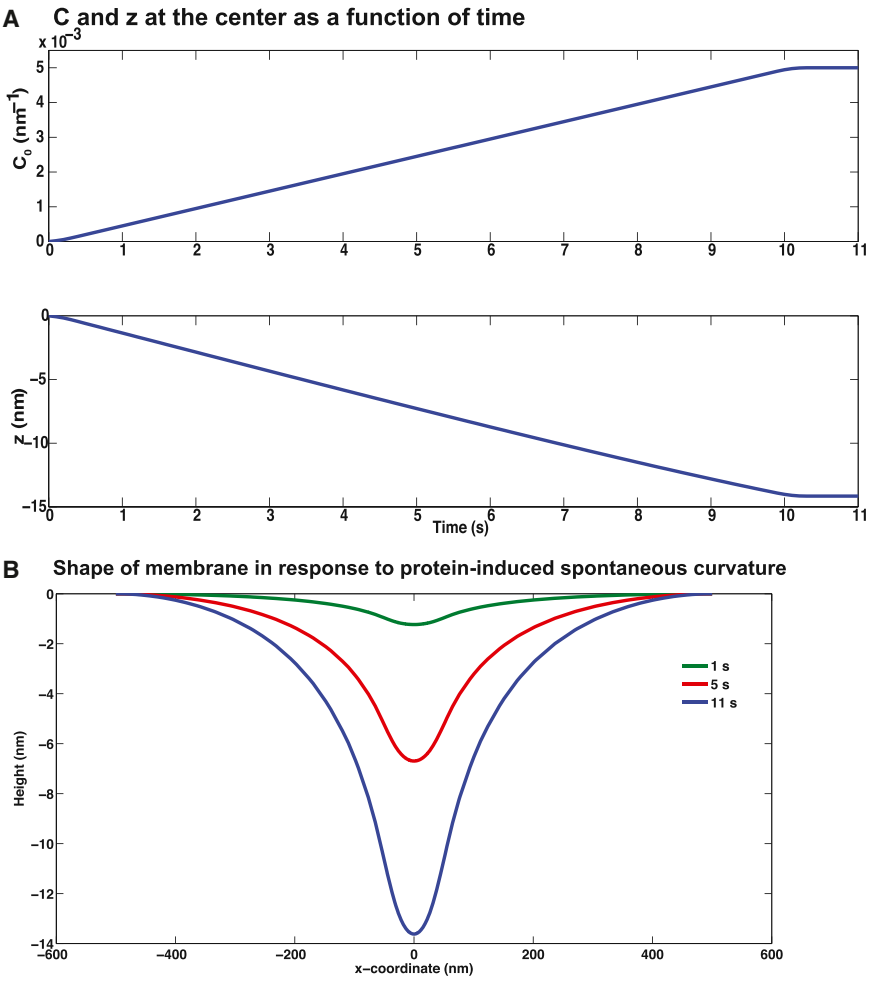

FIGURE 3 The time-dependent change in membrane shape due to protein adsorption. (*A*) Protein-induced spontaneous curvature C and height of the membrane z in the center of the domain as a function of time. (*B*) Shape of the membrane corresponding to line $x^2 = 0$ at three different times. (*C*) An electron micrograph showing an early endocytic invagination (3). To see this figure in color, go online.

COMSOL MULTIPHYSICS (COMSOL, Burlington, MA). Note that all variables appear as second derivatives in space, except for λ, which appears as a first derivative. In order to achieve numerical convergence, we use a linear shape function for λ and quadratic shape functions for the other variables (42–44).

In response to protein adsorption, the shape of the membrane changes with time as shown in Fig. 3 *B*. The height of the deformed membrane in the center is shown in Fig. 3 *A*. Increasing the spontaneous curvature increases the surface area. To accommodate this change, lipids flow in from the open boundaries. As expected, once the spontaneous curvature attains a steady value, the height of the membrane also attains a steady value. The shape of the membrane in response to protein adsorption (Fig. 3 *B*) resembles the early endocytic invagination due to coat protein adsorption (Fig. 3 *C*) (3).

Note that λ is a nonlinear function of the spontaneous curvature C (see Figs. 4 *A* and 3 *A*). Analysis of the local tension profile along the membrane shows that for small values of spontaneous curvature, there is no measurable inhomogeneity in the value of the local tension, λ. As the spontaneous curvature increases, the value of lambda decreases only in the protein patch (Fig. 4 *B*).

The change in λ at the end of protein adsorption process remains a localized effect in the protein patch (Fig. 4). This effect can be explained in part by studying Eq. 14, where the change in λ is given by the first-order partial differential equation. In the region where there are no proteins, $\partial C/\partial x^{\alpha}$

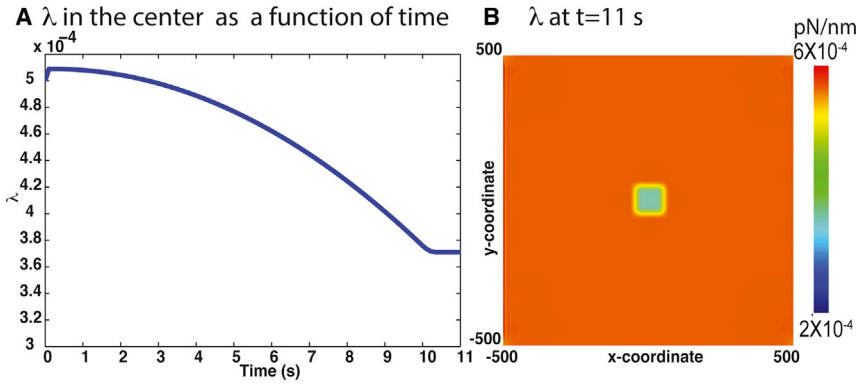

FIGURE 4 Local tension variation on the membrane in response to protein adsorption. (*A*) The value λ versus time in the center of the domain in response to protein adsorption. (*B*) Surface profile of λ at 11 s. To see this figure in color, go online.

goes to zero, and λ is given by the value at the boundary λ_0. At the boundary of the protein adsorption region, the actual mean curvature is less than the applied spontaneous curvature and therefore $H - C \neq 0$. Also,

$$\frac{\partial C}{\partial x^{\alpha}} \neq 0.$$

This implies that the gradient in the tension λ is not zero using Eq. 14. Therefore, there is a jump in the local tension λ at the boundary of the protein patch. In the region containing the proteins, the spontaneous curvature is again uniform and therefore there is no gradient in λ. However, the value of λ is equal to the tension outside the protein patch plus the jump in tension at the boundary, thereby making the change in tension an effect confined to the protein patch.

Effect of protein adsorption area

Because C_0 represents the areal density of proteins on the membrane, increasing the size of the protein patch is tantamount to increasing the total number of proteins on the membrane, while keeping the protein concentration dilute. We studied the effect of increasing the area over which the proteins can adsorb on the membrane for different values of C_0 (Fig. 5). For a given area of protein adsorption, increasing C_0 increases the displacement in the center of the membrane (Fig. 5 *A*) and reduces the value of the membrane tension, λ, in the region (Fig. 5 *B*). Increasing the area over which the proteins can adsorb had a stronger effect on membrane displacement and λ. Note that because λ is a Lagrange multiplier, its value is not restricted to positive values—it can be positive or negative such that the areal incompressibility constraint is satisfied (Eq. 8).

Interaction between two protein patches

As seen in Figs. 3 and 4, protein adsorption leads to a global change in membrane shape and a local change in λ. If one patch of adsorbed proteins causes a local change in λ, then how do two separate regions of proteins interact with one another? In other words, does the change in λ remain confined to regions with adsorbed proteins, or does it propagate across regions with no proteins? To understand this interaction, we performed simulations with two patches of membranes that are placed at different distances apart from one another and studied the evolution of shape and local tension in these systems. The effect of protein binding on to two patches is explained in Figs. S9 and S10. In this case, we explicitly show that although the curvature effects are nonlocal, changes in λ remain localized to the protein patches. Another important result from our work is that when proteins can bind to two patches on the membrane, there is characteristic decay length,

$$\sqrt{\frac{k}{2\lambda}},$$

given by the ratio of out-of-plane bending to the in-plane tension. When the two patches are located at less than or of the same order of magnitude as the decay length, the region between the two patches experiences the curvature changes even though local tension changes are always limited to the patch (see Figs. S9 and S10). When the two patches are much further away, then the curvature between the two patches relaxes to zero in the region between them. Thus, even though the local tension changes remain confined to the patch, the curvature effects are dependent on the characteristic decay length.

Pulling on protein-coated patches

During endocytosis, the first stage is initiation of the endocytic patch by the binding of coat proteins to the membrane, inducing a change in the membrane curvature. Further changes in the membrane shape are generated by localized pulling forces acting on the membrane due to actin polymerization. The effect of protein adsorption shown in Figs. 3, 4, and 5 can be understood as a phenomenological model of coat proteins binding the membranes and reducing the membrane tension.

What is the effect of reducing the membrane tension (i.e., changing λ) on membrane response to forces? We tested the effect of a pulling force localized to the protein-adsorbed

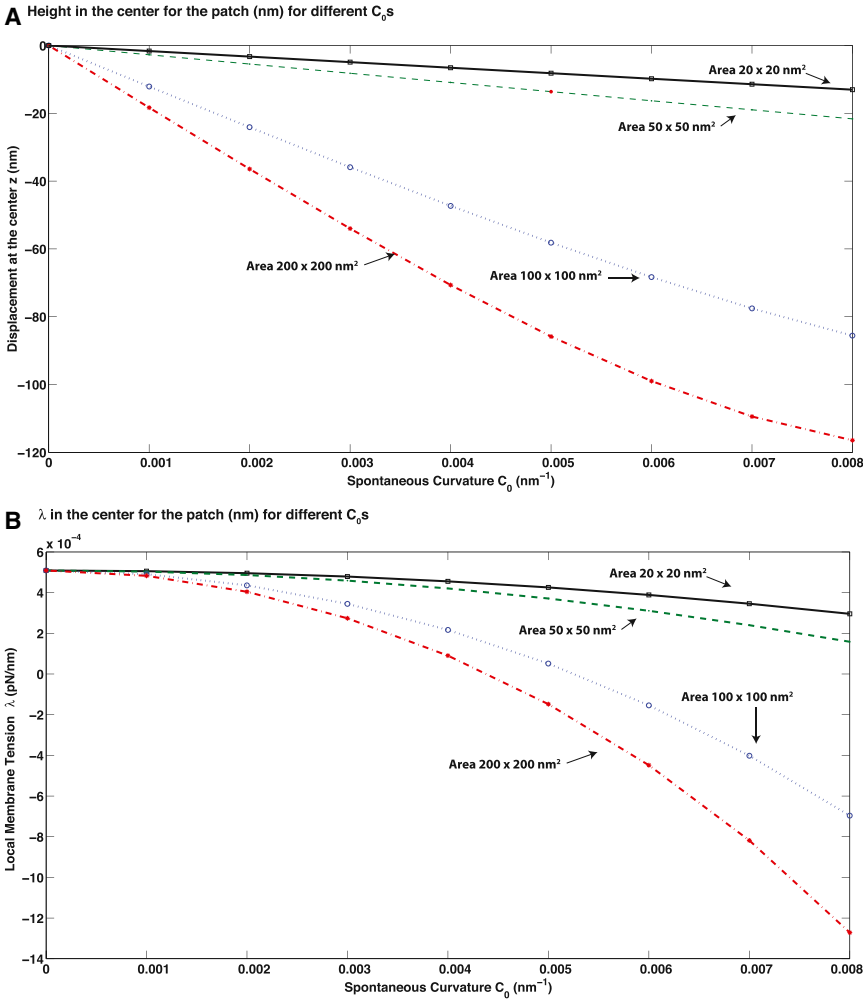

FIGURE 5 Local tension variation on the membrane in response to changing area of protein adsorption. (*A*) The value z versus time in the center of the domain in response to protein adsorption shows that the displacement depends on the area in which proteins can adsorb. (*B*) The value λ also depends on the area of the region in which proteins can adsorb. To see this figure in color, go online.

region for different values of C_0 and for two different areas of protein adsorption (Fig. 6 and see Fig. S7). The pulling force was applied uniformly normal to the protein patch and was held in place after the protein adsorption was complete. In both cases, each value of C_0 shows a different force-displacement relationship, consistent with each system having a different value of λ. Increasing values of C_0 decreased λ in the protein adsorbed region. As the value of λ decreases, less force is required to displace the membrane by a desired amount. This plot can be used to interpret combinations of protein concentrations and forces required to pull the membrane to a desired geometry. For example, to obtain a 200 nm displacement at the center of the membrane (similar to endocytic invaginations in yeast (1)), less force per unit area is required when C_0 is increased. Thus, adsorption of proteins reduces membrane tension and eases further deformation caused by pulling forces.

DISCUSSION AND CONCLUSIONS

Inhomogeneous membranes are the norm rather than the exception in cellular systems. However, contemporary theoretical approaches focus more on the understanding of how homogeneous membranes behave in response to different driving forces such as protein adsorption and pulling forces. Here, we have focused on understanding how inhomogeneous membranes evolve both in shape and surface properties in response to protein adsorption.

We have developed a viscous-elastic model that allows us to simultaneously capture the change in membrane shape and tension in response to protein adsorption. We also show that in two dimensions, the Helfrich model results in an integro-differential equation that is hard to solve when the membrane is inhomogeneous. Introduction of membrane surface viscosity allows us to solve for the change in shape and local tension simultaneously in the case of an inhomogeneous membrane. This situation is of particular biological relevance: there are many cases where protein binding or membrane crowding is localized (2–5).

The adsorption of proteins to specific membrane microdomains is often the first step in a biological process like endocytosis. In many of these processes, the local regions where proteins bind are also regions where further shape changes take place. For example, in endocytosis, the early

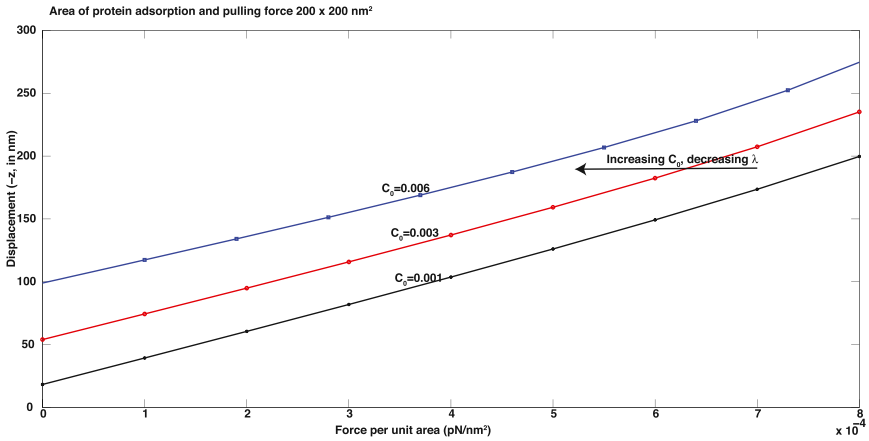

FIGURE 6 Effect of a pulling force localized to the region where the proteins are adsorbed. The displacement of the membrane depends on the area and density of proteins (C_0). Increasing C_0 decreases the membrane tension λ and the force-displacement curve is shifted such that when λ decreases, less force is required to achieve a given displacement. Protein and pulling region are 200 $\times$ 200 nm^2. To see this figure in color, go online.

invagination is followed by tubulation and subsequent scission of the vesicle. In Fig. 3, we show how the spontaneous curvature of the proteins adsorbing on the membrane leads to a change in the shape of the membrane that is similar in size and shape to that of an early endocytic invagination. Our model and simulations also show that the change in shape is accompanied by a change in the local tension of the membrane in the local region where proteins are bound (Fig. 4). The change in local tension depends on the area over which the proteins are adsorbed (Fig. 5), suggesting that protein curvature and area of coverage regulates not only membrane curvature but also local tension.

It is possible that the lowering of local tension of the membrane will have a functional impact on downstream effects of protein binding. In fact, one experimentally testable prediction from our work is that protein adsorption on the membrane can lower the local tension and the energy barrier for subsequent events in that region. If this is the case, then the protein-coated membrane will deform more for the same applied force when compared to the uncoated bare membrane. Our simulations show that the force response behavior of the protein-coated membrane depends on the change in local tension induced by protein-adsorption. In order to obtain a given displacement, less force is needed when the membrane tension is lowered by protein adsorption (Fig. 6).

Experiment design

The cellular milieu is crowded, with peripheral and transmembrane proteins, and cytoskeleton and intracellular organelles. Thus, one of the experimental challenges is deciphering the separate roles of the membrane and its resident proteins. However, the results of our work can be tested experimentally in giant unilamellar vesicles, as shown in Fig. 1 for both homogeneous and inhomogeneous vesicles.

Pipette aspiration, in conjunction with bead pulling experiments, can be used to test the predictions of our model. Specifically, by following the experimental procedure outlined in Heinrich et al. (45), pipette aspiration can be used to control the initial membrane tension and our model can be used to quantify the changes in the local tension due to bead pulling. Separately, in Singh et al. (46), it has been suggested that increase in protein concentration needs less force in stabilizing the tether, once it is formed. This is similar to the observations made in Fig. 6. These experimental studies are along the lines of our modeling efforts.

One proposed experiment is to coat an entire vesicle with a curvature-inducing protein of known properties and study the change in size. The change in the radius of the vesicle can be used to estimate the change in membrane tension assuming Laplace's equation. Another proposed experiment is to localize tether pulling to a phase-separated domain on the membrane and estimate change in the membrane tension locally. In both these cases, pulling tethers out of the protein-coated region (also see Interpretation of Membrane Tension) will allow us to estimate the change in tension and these results can be compared against the force response curves shown in Fig. 6.

While these experiments are easy enough to design theoretically, we are aware that there might be technical challenges in performing them. One challenge is purifying sufficiently large quantities of protein to coat an entire giant unilamellar vesicle and obtaining high coverage of the vesicle surface with proteins. Another is the difficulty in measuring the radius of the vesicle before and after protein adsorption with high resolution. Discussion with our experimental colleagues indicated that pulling tethers locally in a confined region may be fairly challenging. Nonetheless, we have described these experiments in the hope that as more sophisticated technologies emerge, it is but a matter of time before these experiments can be conducted.

Open questions for the future

We have developed our model based on certain assumptions, as outlined above. Here, we identify some of the limitations of the model and open questions for future study, while

noting that none of our assumptions have prevented us from obtaining the results we sought. Our model is based on a single manifold to represent a bilayer. This model can be extended to included two manifolds, one for each monolayer. Then, in addition to lipid flow on each monolayer, we would need to include interleaflet friction. Including intermonolayer friction and bulk liquid viscosity (22,23) along with membrane surface viscosity may also be necessary to accurately model membrane behavior in response to local inhomogeneities.

It is likely that, in addition to lipid flow, inclusion of lipid and protein diffusion will further impact the surface properties of the membrane. It should also be noted that proteins can induce both spontaneous mean and Gaussian curvature. Even if we were to include a spontaneous Gaussian curvature (similar to Seguin and Fried (47) and Kim et al. (48)) in the energy (Eq. 17), a viscous-elastic formulation would still be necessary to describe the system uniquely. These issues will be addressed in a future study.

SUPPORTING MATERIAL

Supporting Materials and Methods, 26 equations, and 10 figures are available at http://www.biophysj.org/biophysj/supplemental/S0006-3495(14)00616-X.

We thank Profs. David Steigmann, Panos Papadopoulos, and Dr. Yidi Sun for many useful discussions.

We acknowledge funding from the National Institutes of Health (grant No. R01GM104979) to G.O. and the University of California at Berkeley Chancellor's Postdoctoral Fellowship to P.R.

REFERENCES

1. Kukulski, W., M. Schorb, …, J. A. G. Briggs. 2012. Plasma membrane reshaping during endocytosis is revealed by time-resolved electron tomography. *Cell.* 150:508–520.
2. Kishimoto, T., Y. Sun, …, D. G. Drubin. 2011. Determinants of endocytic membrane geometry, stability, and scission. *Proc. Natl. Acad. Sci. USA.* 108:E979–E988.
3. Buser, C., and D. G. Drubin. 2013. Ultrastructural imaging of endocytic sites in *Saccharomyces cerevisiae* by transmission electron microscopy and immunolabeling. *Microsc. Microanal.* 19:381–392.
4. Walther, T. C., J. H. Brickner, …, P. Walter. 2006. Eisosomes mark static sites of endocytosis. *Nature.* 439:998–1003.
5. Karotki, L., J. T. Huiskonen, …, T. C. Walther. 2011. Eisosome proteins assemble into a membrane scaffold. *J. Cell Biol.* 195:889–902.
6. Stachowiak, J. C., E. M. Schmid, …, C. C. Hayden. 2012. Membrane bending by protein-protein crowding. *Nat. Cell Biol.* 14:944–949.
7. Arkhipov, A., Y. Yin, and K. Schulten. 2008. Four-scale description of membrane sculpting by BAR domains. *Biophys. J.* 95:2806–2821.
8. Valentine, C. D., and P. M. Haggie. 2011. Confinement of β_1- and β_2-adrenergic receptors in the plasma membrane of cardiomyocyte-like H9c2 cells is mediated by selective interactions with PDZ domain and A-kinase anchoring proteins but not caveolae. *Mol. Biol. Cell.* 22:2970–2982.
9. Olivera-Couto, A., M. Graña, …, P. S. Aguilar. 2011. The eisosome core is composed of BAR domain proteins. *Mol. Biol. Cell.* 22:2360–2372.
10. Frost, A., R. Perera, …, V. M. Unger. 2008. Structural basis of membrane invagination by F-BAR domains. *Cell.* 132:807–817.
11. Ohki, S., G. A. Baker, …, F. V. Bright. 2006. Interaction of influenza virus fusion peptide with lipid membranes: effect of lysolipid. *J. Membr. Biol.* 211:191–200.
12. El Alaoui Faris, M. D., D. Lacoste, …, P. Bassereau. 2009. Membrane tension lowering induced by protein activity. *Phys. Rev. Lett.* 102:038102.
13. Manneville, J. B., P. Bassereau, …, J. Prost. 2001. Active membrane fluctuations studied by micropipet aspiration. *Phys. Rev. E Stat. Nonlin. Soft Matter Phys.* 64:021908.
14. Helfrich, W., and R. M. Servuss. 1984. Undulations, steric interaction and cohesion of fluid membranes. *Il Nuovo Cimento D.* 3:137–151.
15. Lipowsky, R. 2013. Spontaneous tubulation of membranes and vesicles reveals membrane tension generated by spontaneous curvature. *Faraday Discuss.* 161:305–331, discussion 419–459.
16. Zhao, H., A. Michelot, …, P. Lappalainen. 2013. Membrane-sculpting BAR domains generate stable lipid microdomains. *Cell Reports.* 4:1213–1223.
17. Baumgart, T., S. T. Hess, and W. W. Webb. 2003. Imaging coexisting fluid domains in biomembrane models coupling curvature and line tension. *Nature.* 425:821–824.
18. Fischer, T. M. 1992. Is the surface area of the red cell membrane skeleton locally conserved? *Biophys. J.* 61:298–305.
19. Raucher, D., and M. P. Sheetz. 1999. Characteristics of a membrane reservoir buffering membrane tension. *Biophys. J.* 77:1992–2002.
20. Secomb, T. W., and R. Skalak. 1982. A two-dimensional model for capillary flow of an asymmetric cell. *Microvasc. Res.* 24:194–203.
21. Secomb, T. W., and R. Skalak. 1982. Surface flow of viscoelastic membranes in viscous fluids. *Q. J. Mech. Appl. Math.* 35:233–247.
22. Seifert, U., and S. A. Langer. 1993. Viscous modes of fluid bilayer membranes. *Europhys. Lett.* 23:71.
23. Fournier, J.-B., N. Khalifat, …, M. I. Angelova. 2009. Chemically triggered ejection of membrane tubules controlled by intermonolayer friction. *Phys. Rev. Lett.* 102:018102.
24. Arroyo, M., and A. Desimone. 2009. Relaxation dynamics of fluid membranes. *Phys. Rev. E Stat. Nonlin. Soft Matter Phys.* 79:031915.
25. Rangamani, P., A. Agrawal, …, D. J. Steigmann. 2013. Interaction between surface shape and intra-surface viscous flow on lipid membranes. *Biomech. Model. Mechanobiol.* 12:833–845.
26. Rahimi, M., and M. Arroyo. 2012. Shape dynamics, lipid hydrodynamics, and the complex viscoelasticity of bilayer membranes [corrected]. *Phys. Rev. E Stat. Nonlin. Soft Matter Phys.* 86:011932.
27. Sens, P. 2004. Dynamics of nonequilibrium membrane bud formation. *Phys. Rev. Lett.* 93:108103.
28. Helfrich, W. 1973. Elastic properties of lipid bilayers: theory and possible experiments. *Z. Naturforsch. C.* 28:693–703.
29. Kwok, R., and E. Evans. 1981. Thermoelasticity of large lecithin bilayer vesicles. *Biophys. J.* 35:637–652.
30. Sokolnikoff, I. S. 1964. Tensor Analysis: Theory and Applications to Geometry and Mechanics of Continua. John Wiley, New York.
31. Steigmann, D. J. 1999. Fluid films with curvature elasticity. *Arch. Ration. Mech. Anal.* 150:127–152.
32. Jenkins, J. T. 1977. Static equilibrium configurations of a model red blood cell. *J. Math. Biol.* 4:149–169.
33. Derényi, I., F. Jülicher, and J. Prost. 2002. Formation and interaction of membrane tubes. *Phys. Rev. Lett.* 88:238101.
34. Phillips, R., J. Kondev, and J. Theriot. 2009. Physical Biology of the Cell. Garland Science, New York.
35. Pécréaux, J., H. G. Döbereiner, …, P. Bassereau. 2004. Refined contour analysis of giant unilamellar vesicles. *Eur. Phys. J. E Soft Matter.* 13:277–290.

36. Siegel, D. P., and M. M. Kozlov. 2004. The Gaussian curvature elastic modulus of *n*-monomethylated dioleoylphosphatidylethanolamine: relevance to membrane fusion and lipid phase behavior. *Biophys. J.* 87:366–374.

37. Siegel, D. P. 2006. Determining the ratio of the Gaussian curvature and bending elastic moduli of phospholipids from Q_{II} phase unit cell dimensions. *Biophys. J.* 91:608–618.

38. Hu, M., J. J. Briguglio, and M. Deserno. 2012. Determining the Gaussian curvature modulus of lipid membranes in simulations. *Biophys. J.* 102:1403–1410.

39. Agrawal, A., and D. J. Steigmann. 2009. Modeling protein-mediated morphology in biomembranes. *Biomech. Model. Mechanobiol.* 8: 371–379.

40. Zhu, C., S. L. Das, and T. Baumgart. 2012. Nonlinear sorting, curvature generation, and crowding of endophilin N-BAR on tubular membranes. *Biophys. J.* 102:1837–1845.

41. Zienkiewicz, O. C., and R. L. Taylor. 2000. The Finite Element Method: Solid Mechanics, Vol. 2. Butterworth-Heinemann, Woburn, MA.

42. Hughes, T. J. R., F. P. Leopoldo, and M. Balestra. 1986. A new finite element formulation for computational fluid dynamics: V. Circumventing the Babuška-Brezzi condition: a stable Petrov-Galerkin formulation of the Stokes problem accommodating equal-order interpolations. *Comput. Methods Appl. Mech. Eng.* 59:85–99.

43. Bathe, K. J. 1996. Finite Element Procedures. Prentice-Hall, Englewood Cliffs, NJ.

44. Babuska, I. 1973. The finite element method with Lagrangian multipliers. *Num. Math.* 20:179–192.

45. Heinrich, M., A. Tian, …, T. Baumgart. 2010. Dynamic sorting of lipids and proteins in membrane tubes with a moving phase boundary. *Proc. Natl. Acad. Sci. USA.* 107:7208–7213.

46. Singh, P., P. Mahata, …, S. L. Das. 2012. Curvature sorting of proteins on a cylindrical lipid membrane tether connected to a reservoir. *Phys. Rev. E Stat. Nonlin. Soft Matter Phys.* 85:051906.

47. Seguin, B., and E. Fried. 2014. Microphysical derivation of the Canham-Helfrich free-energy density. *J. Math. Biol.* 68:647–665.

48. Kim, K. S., J. Neu, and G. Oster. 1998. Curvature-mediated interactions between membrane proteins. *Biophys. J.* 75:2274–2291.

49. Lipowsky, R., and E. Sackmann. 1995. Structure and Dynamics of Membranes. Elsevier, Amsterdam, The Netherlands.

50. Hochmuth, R. M., and R. E. Waugh. 1987. Erythrocyte membrane elasticity and viscosity. *Annu. Rev. Physiol.* 49:209–219.

51. Dimova, R., S. Aranda, …, R. Lipowsky. 2006. A practical guide to giant vesicles. Probing the membrane nanoregime via optical microscopy. *J. Phys. Condens. Matter.* 18:S1151–S1176.